# Determination of acousto-ultrasonics wave propagation in an isotropic Al6082-T6 plate: Experimental and analytical investigations

Kumar Shantanu Prasad [1, *], Gbanaibolou Jombo [1], Sikiru Oluwarotimi Ismail [1], Yong Kang Chen [1] and Hom Nath Dhakal [2]

[1] *Centre for Engineering Research, School of Physics, Engineering and Computer Science, University of Hertfordshire, AL10 9AB, Hatfield, UK.*
[2] *Advanced Polymers and Composites (APC) Research Group, School of Mechanical and Design Engineering, University of Portsmouth, PO1 3DJ, Portsmouth, UK.*

World Journal of Advanced Engineering Technology and Sciences, 2024, 13(01), 621–630

Publication history: Received on 12 August 2024; revised on 26 September 2024; accepted on 29 September 2024

Article DOI: https://doi.org/10.30574/wjaets.2024.13.1.0456

## Abstract

The ability to guarantee reliable and damage-tolerant operation of structures is critical to their safe operation. Various non-destructive evaluation (NDE) techniques, such as ultrasonics, acoustic emission, thermography, acousto-ultrasonics (AU), among others, provide a means of inspecting cracks, defects and damage responses in structures. AU technique involves active excitation of a structure, using ultrasonic waves when accessing defects, damage and mechanical property variation based on acoustic emission sensing and analysis. The focus of previous works has been on experimental understanding of the relationship between propagating AU wave attenuation parameters and various defects, damage and mechanical property variation without establishing fundamental AU wave propagation problems. Therefore, the objective of this paper is to provide an understanding of the physical problem of AU wave propagation through an isotropic plate and its analytical validation, using wave dispersion concept. The experimental investigation was conducted on Al6082-T6 plate specimen. Wave propagation speed on upper and lower surfaces of the specimen was investigated. The changes of the wave speed and attenuation with frequency were identified. From the results obtained experimentally, the wave dispersion was verified analytically. Also, Lamb waves were discovered to be the dominating AU waves. The wave was appreciably non-dispersive in the frequency range from 150 to 1000 kHz and the attenuation coefficient was increased with the frequency. This finding provides a breakthrough to the implementation of Acousto- ultrasonics in the non- destructive testing applications such as to possibly access the damages in the wind turbine blade composite structures as AU has the active sensing mechanism providing an edge over AE method which is a passive mode of damage sensing.

**Keywords:** Acousto-ultrasonics (AU); Non-destructive evaluation (NDE); Wave propagation; Wave dispersion

## 1. Introduction

Acousto-ultrasonics (AU) is a non-destructive testing and structural assessment technique that integrates acoustic emission (AE) methods with ultrasonic excitation of stress waves [1]. AU is a type of inspection methodology that is used to detect and analyse defect and damage in structures [2]. AU is strongly linked with AE methodology. AU can be defined as AE that has been simulated or facilitated by ultrasonic sources. The big distinction between AU and AE techniques is the nature of exciting the elastic stress waves; AE approach relies on structural loading to generate immediate and spontaneous stress waves, while AU adopts ultrasonic waves as external pulsers [3]. In an isotropic material, during the wave propagation, the particle displacement is either parallel or transverse to the direction of the

* Corresponding author: Kumar Shantanu Prasad

wave propagation. When the wavelength approaches the plate thickness, the wave velocities are function of frequency (dispersion) [4].

Lamb or plate waves are produced in relatively thin isotropic material plates or anisotropic laminates [5–7]. The injection of a longitudinal wave onto the specimen's surface results to leaky surface waves [8,9]. Although Lamb waves can be considered dispersive in nature [10,11], mostly due to out-of-plane/anti-symmetric modes; however, under low-frequency approximations (200 kHz- 1 MHz), Lamb waves can exhibit non-dispersive symmetric modes and a dispersive anti-symmetric modes [12,13], and the Lamb wave propagation behaviour can possibly be described by the use of dispersion curves [14], which are plots of phase velocities against the product of frequency and thickness created by computing the Lamb wave equations. The dispersion in this case is created by the plate's borders and is referred to as geometrical dispersion. Lamb waves may operate in two different modes, symmetric ($S_n$) and antisymmetric ($A_n$), which can transmit separately or simultaneously. The notation, *n* indicates the mode order or the count of inflexion points along the thickness of specimen.

Furthermore, Lamb waves dispersion behaviours have been stated in some studies. Following the first tests by Fredrik and Worlton [15], plate waves have been investigated. Worlton [16] reported on empirical investigation of dispersive lamb waves for zirconium. Moving forward, plate waves especially in relation to smart structures with permanently implanted or attached sensors are relevant to the structural health monitoring (SHM) industry, including the research based on the Lamb wave dispersion equations proposed by Viktorov [6] and Rose [17].

However, lamb waves application and propagation characteristics in AU technique is still at the initial phase of research. Hence, it is important to investigate into the AU wave propagation behaviour in an isotropic plate structure for a deeper understanding. This is also necessary because it fluctuates between multiple reflections at the top and bottom surfaces, as well as some mutual interference [18]. In general, both dispersion and attenuation occur in a medium during longitudinal and shear wave propagation [19–22]. When transmitting in a dispersive and attenuating environment, both amplitude and frequency level of the wave might constantly change [23]. Hence, this paper presents experimental and analytical investigations focusing on better understanding of the Lamb wave propagation in an isotropic Al plate, using AU techniques.

## 2. Material and methods

### 2.1. Specimen

The experiment was demonstrated on Al 6082-T6 plate specimen. Table 1 highlights the dimension and mechanical properties of the specimen used.

**Table 1** Properties and dimension of the material (specimen) used [24]

| Material | Dimension (mm) | Elastic modulus, E (MPa) | Shear modulus, G (MPa) | Tensile strength, $\sigma_T$ (MPa) | Poisson ratio ($\upsilon$) | Density ($\rho$) (g/cm$^3$) | Longitudinal velocity, $V_L$ (m/s) | Transverse velocity, $V_T$ (m/s) |
|---|---|---|---|---|---|---|---|---|
| Al 6082-T6 | 200 *x* 150 *x* 2 | 72000 | 33800 | 270 | 0.33 | 2.70 | 6100-6320 | 2900-3100 |

### 2.2. Experimental set-up

The schematic representation of the AU configuration and its actual experimental set-up are shown in Figs 1 and 2, respectively.

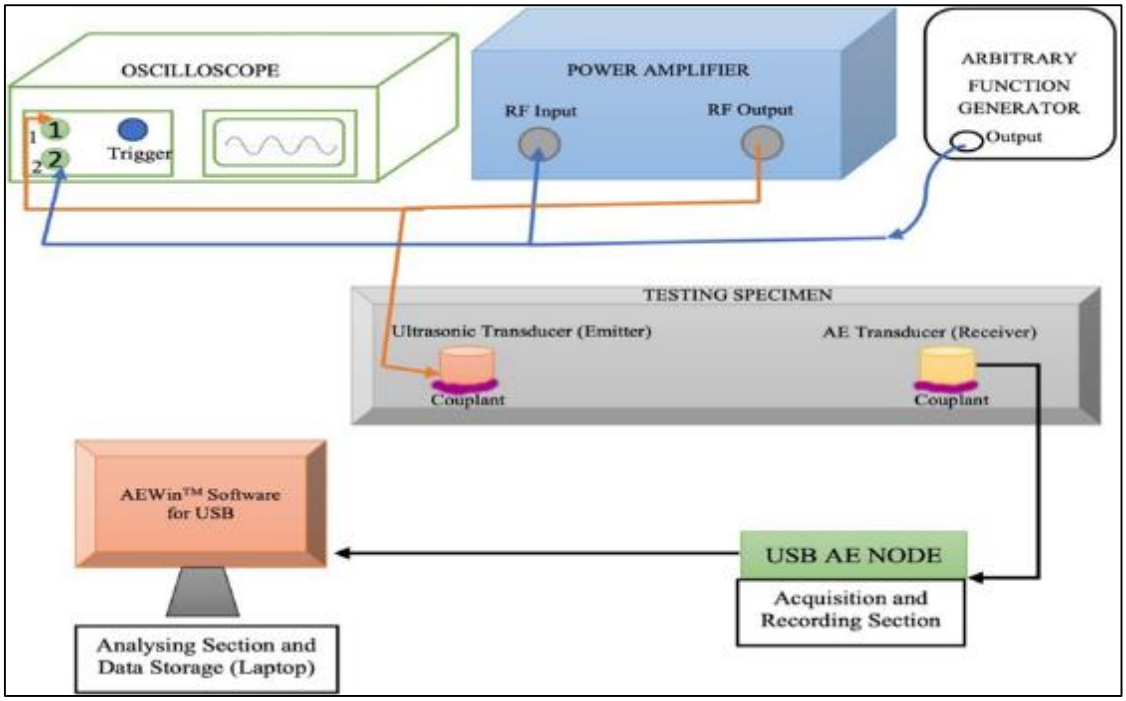


**Figure 1** Schematic representation of AU configuration

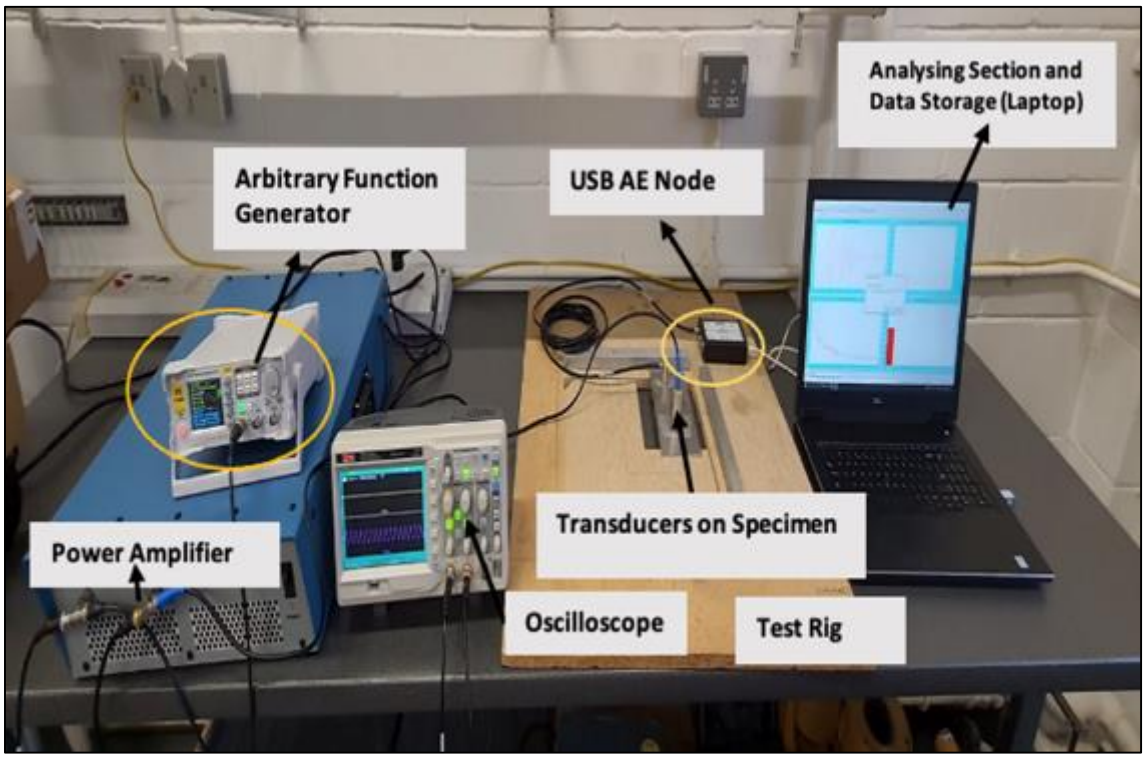


**Figure 2** Actual AU exeperimental set-up

An analytical model which addresses the plate wave propagation, focusing on the measurement of the lamb wave velocity (dispersion curves) was developed, using MATLAB. The specimen was supported on a test rig with the spacing in-between to support the testing specimen on its edges and eliminate any interference with the support structure when transmitting and receiving signal. An ultrasonic piezo-electronic transducer of 1 MHz and a resonant-type AE transducer with resonant frequency of 150 MHz were used as an emitter and a receiver, respectively. The details on the transducers

are presented in Table 2. The transducers were bonded to the specimen with a wax, acting as a couplant. A contact pressure of 0.072 MPa was maintained between the sensor and the testing specimen throughout a test. To drive and send the signal to the ultrasonic transducer, an arbitrary function generator was used to generate a 3-cycle sine wave tone burst manual signals with the peak-to-peak amplitude of 15.8 mV. This signal was then transmitted to a power amplifier of 50 dB to amplify the sending signal to a peak-to-peak amplitude of 5 V. Both signals, before and after the power amplifier, were analysed in the oscilloscope.

**Table 2** Operating features of the emitting and receiving transducers

| **Feature** | **Type of sensor** | |
|---|---|---|
| | **Emitter (ultrasonic piezo-electronic transducer)** | **Receiver (resonant-type AE transducer)** |
| Resonant/centre frequency (kHz) | 1000 | 150 |
| Operating frequency range (kHz) | --- | 50-750 |
| Weight (grams) | --- | 34 |
| Transducer diameter (mm) | 23 | 19 |

More also, on the receiver's end, the narrow band resonant-type AE sensor which has a flat frequency response up to 750 kHz, with a resonant peak at 150 kHz, was connected to the AE signal acquisition system configured with a sampling rate of 5 MHz. Additionally, an analogue and a digital Butterworth bandpass filters covering the frequency range from 20 to 1 MHz and 80 to 100 kHz respectively were configured to avoid the insertion of ambient sound in the AU acquired signal. Fig. 3 shows the schematic representation of the sensor placements for velocity and attenuation measurements.

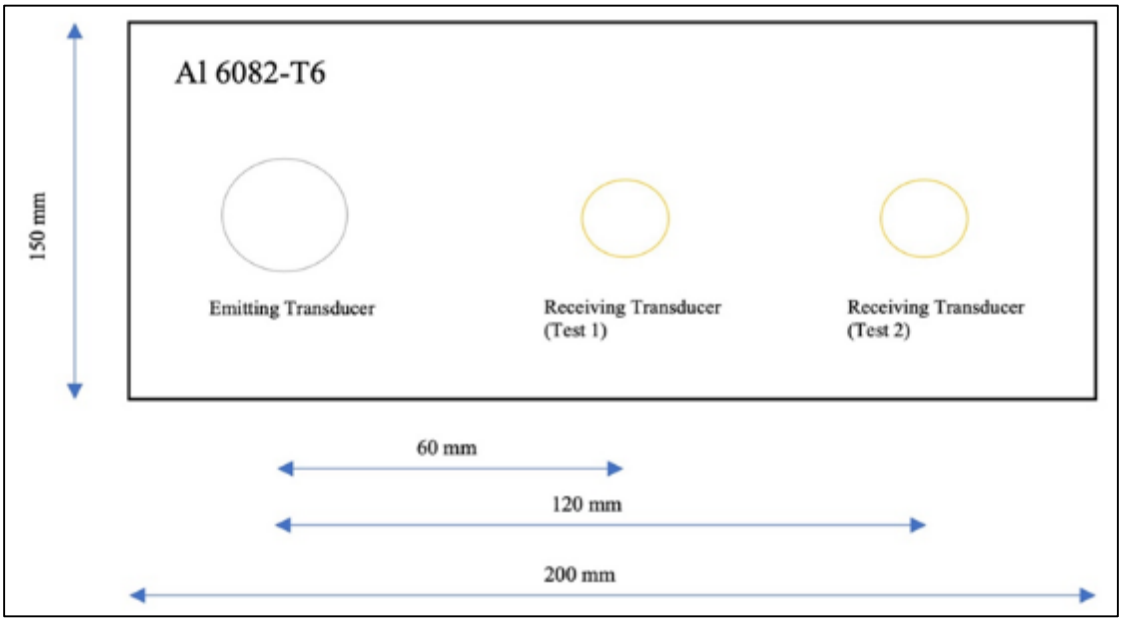


**Figure 3** The diagrammatic illustration of sensor placements for velocity and attenuation measurements

When acquiring AU wave data, the signal characterisation constraints were created similarly to those found in [25,26]:

- Peak definition time (PDT): 3000 µs
- Hit definition time (HDT): 600 µs
- Hit lockout time (HLT): 1000 µs

Furthermore, two sets of experiment were taken with a varying frequency range of 150 - 1000 kHz for each surface of the Al6082-T6 plate, considering upper and the lower surfaces. The two sets of experiment referred to the two different sets of emitter and receiver sensor distance. The sensor distance was chosen wisely to avoid any reflection of the wave.

The receiver's transducer was placed at the positions of 60 and 120 mm from the emitting transducer. The velocity was then determined by utilising these sensors spacing distance in accordance with the report of Kiernan [27]. The frequency-domain (fast Fourier transform) of the signal was also analysed.

The average values were used to estimate the attenuation coefficients, which were obtained using Eq. (1) [28].

$$r(w) = [ln(V_1/V_2)]/(X_2 - X_1) \quad \text{..... (1)}$$

where $r$, $V_1$ and $V_2$ denote attenuation coefficient, peak amplitudes at $X_1$ (60 mm) and $X_2$ (120 mm) sensor spacing.

### 2.3. Analytical method

Experimentally, the phase velocity of the wave propagation was obtained by using the method proposed by Kiernan [27], governed by Eq. (2).

$$V_{ph} = \Delta d/\Delta t \quad \text{..... (2)}$$

where $V_{ph}$, Δd and Δt represent the phase velocity (mm/sec), difference in the sensor spacings (mm) and time difference (sec), respectively. The $\Delta t$ was calculated by tracing a same phase point on the waveform showing at the output for both sensor spacing at 60 and 120 mm. While $\Delta d$ was determined by measuring the displacement of the sensor spacing, which was obtained as 60 mm.

Analytically, according to the Rayleigh-Lamb frequency equations, the dispersion relation of the two modes for an isotropic plate with a thickness of $2h$ is controlled by the following expressions/Eqs (3a) and (3b) [17]:

$$(k^2 - q^2)\, tan(qh) + 4k^2pq\, tan(ph) = 0 \quad \text{(symmetric modes) ..... (3a)}$$

$$(k^2 - q^2)\, tan(ph) + 4k^2pq\, tan(qh) = 0 \quad \text{(anti-symmetric modes) ..... (3b)}$$

where $k$ denotes the wave number. It is numerically represented as $\omega/V_{ph}$, $\omega$ and $V_{ph}$ stand for the angular frequency and phase velocity, respectively. The coefficients, $p^2 = \omega^2/V_L{}^2$ and $q^2 = \omega^2/V_T{}^2$ are given by Rose [17], where $V_L$ and $V_T$ represent the longitudinal and transverse wave velocities, respectively. Both Eqs (3a) and (3b) as well as values in Table 1 were utilised to create a dispersion relation tool/analytical model in MATLAB.

## 3. Results and discussion

### 3.1. Plate wave propagation with dispersion: Analytical verification

Two popular techniques can be utilised to produce a Lamb wave in a plate. The wedge approach is one of the techniques. This approach involves activation of the plate, using ordinary fluctuations generated by a transducer linked acoustically to the testing specimen's surface [5,6]. The second technique is a broadband methodology in which all potential modes for a particular frequency are generated simultaneously, as symmetric and anti-symmetric modes. The latter strategy was utilised in this experiment in accordance with the AU technique configuration, as previously shown in Fig. 1. Lamb waves propagated on a surface possess a velocity component that was both longitudinal and perpendicular to the material's surface. According to the symmetric mode of motion, any particle motion is symmetric about the mid-plane of the plate. The longitudinal movements are equal in magnitude and direction, whereas transverse displacements are identical in magnitude although in the reverse direction. This mode features the particle motion that is antisymmetric with respect to the mid-plane of the plate, hence it is called the anti-symmetric mode [5]. In this investigation, fundamental symmetric ($S_o$) and anti- symmetric plate modes were studied. They were easily generated and received with enough selectivity above the cut-off frequencies of the higher modes [29,30].

With AU approach, three-cycle sine wave tone burst signals were transmitted into the material, using an ultrasonic transducer operating in the frequency range from 150 kHz to 1 MHz. The response of an isotropic material at low frequencies was of main concern in this study.

Moreover, the plate wave velocities at different frequencies for Al6082-T6 specimen were calculated, using Eq. (3a) and the results obtained are shown in Fig. 4. It was evident that from the analytical results that the symmetric wave velocity reduced as the frequency increased, but the anti-symmetric wave velocity increased as the frequency increased, as observed in Fig. 5. To identify a general principle of wave propagation in the AU technique, there should not be

any significant dispersion of the symmetric mode velocity with frequency. According to the analytical model, there is only a 5.38 % decrease in velocity over the frequency range of 150 kHz to 1 MHz, which is a small drop. As a result, in the frequency range under consideration, the symmetric mode is practically non-dispersive. The antisymmetric mode velocity, on the other hand, cannot be greater than the symmetric mode velocity.

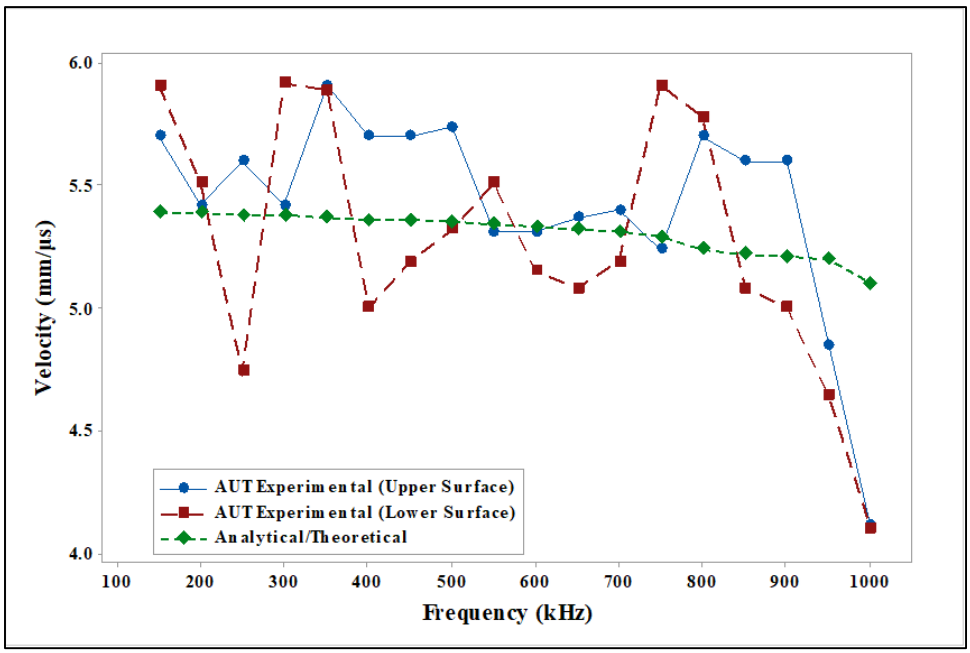


**Figure 4** Dispersion of the symmetric plate wave velocity with frequency

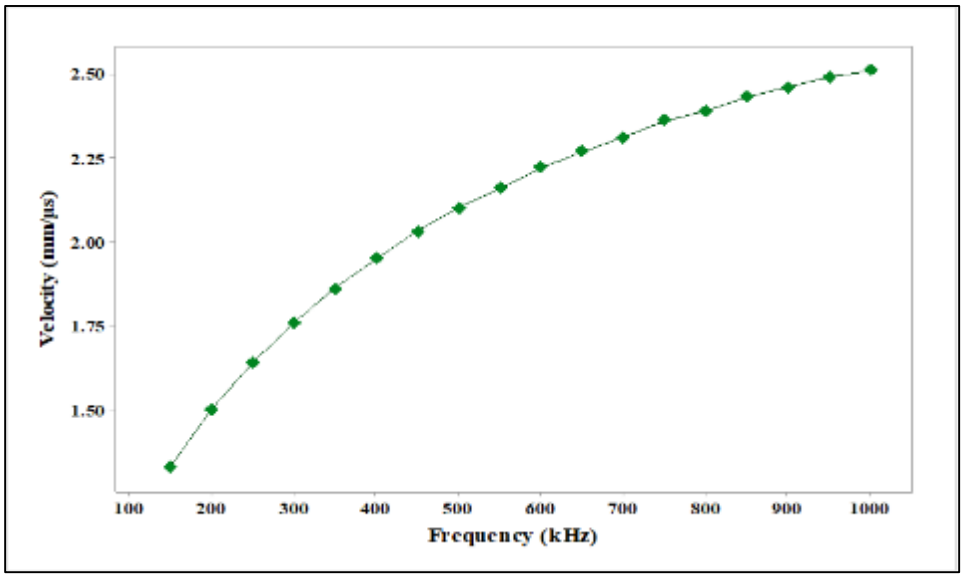


**Figure 5** Dispersion of the anti-symmetric plate wave velocity with frequency

From the experimental results, similar pattern can be obtained. The observed velocities in the specimen for a frequency range from 150kHz to 1 MHz are shown in Fig. 4. From the readings, dispersion of symmetric modes for both the surfaces was calculated and compared with the model. The values obtained experimentally were lower than those expected analytically. The experimental average values were around 6.7% lower than analytical results. Similarly, the trend was the same in both within the same frequency range. Hence, symmetric mode was almost non-dispersive in the frequency range studied. Also, the out-of-plane propagation velocity of the plate wave was the same on the top surface of the wave as that on the bottom surface. To determine whether this was valid or not, the whole series of experiments

were performed or repeated on the opposite surface of the specimen. The same contact pressure of 0.072 MPa was maintained throughout the process. The observed velocities on the lower and upper surfaces of the specimen were nearly identical (Fig. 4).

As depicted in Fig. 6, the peak amplitudes were identical on both bottom and top surfaces of the plate. The attenuation was responsible for the decrease in peak amplitude, as the frequency of the signal increased. Therefore, it can be stated that a plate wave was produced under the AU configuration and experimental set-up, as shown in Figs 1 -2, respectively.

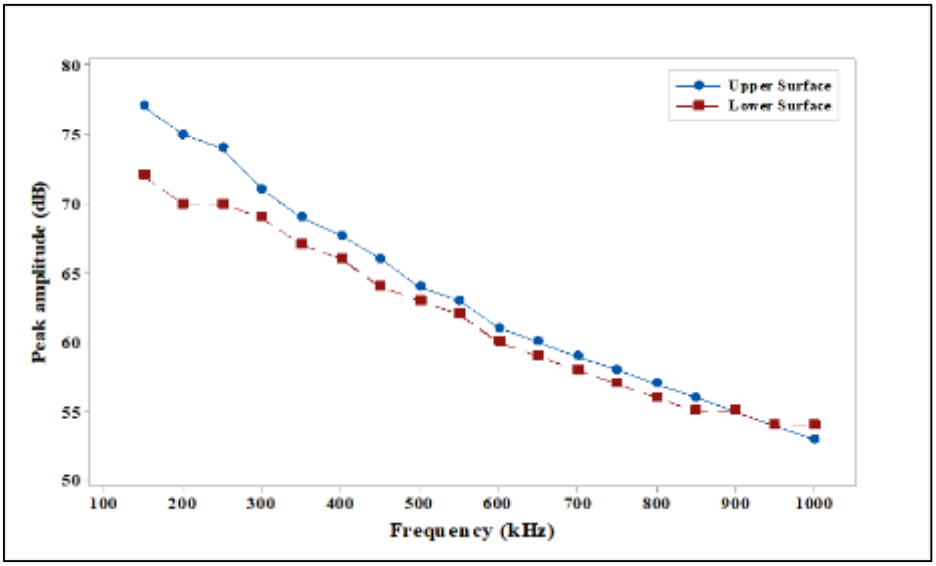


**Figure 6** Peak amplitude of received wave on both upper and lower surfaces of the Al6082- T6 specimen

Moving forward, the centroid frequency of the received signal was nearly exactly the same as the input signal on both surfaces (Fig. 7). The fast Fourier transform spectrum of the received signal revealed that all frequency portions were eliminated with exception of the central frequency. Consequently, it can be inferred that the wave travelled through the material without exhibiting any significant dispersion in the frequency range under consideration.

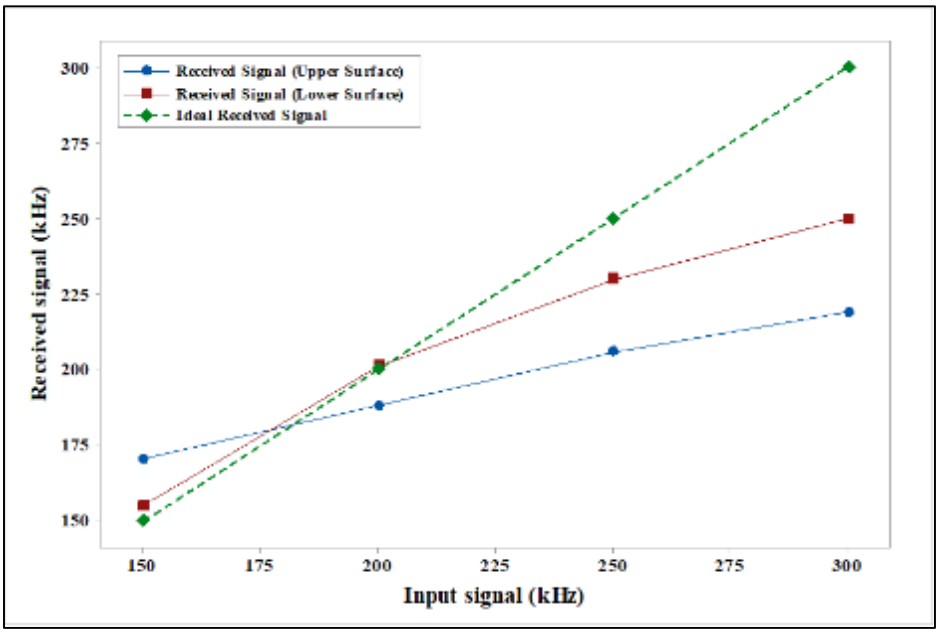


**Figure 7** Variation in the frequency of received wave with emitted wave

Fig. 8 shows that the wavelength of the Lamb wave decreased as the frequency increased Over the studied frequency range, the wavelength decreased from 27.08 to 3.92 mm and 23.40 to 4.10 mm for the top and lower surfaces,

respectively. Nonetheless, the lowest wavelength was higher than the plate thickness of 2 mm, demonstrating the validity of the experiment. Besides, at the input frequency of 200 kHz, the wavelengths were 17.57mm and 15.60 mm for the upper and lower surfaces, respectively. These data are relevant to pick a defect detection frequency for the material, since the capacity of the technique to detect flaws increased as the wavelength decreased [28].

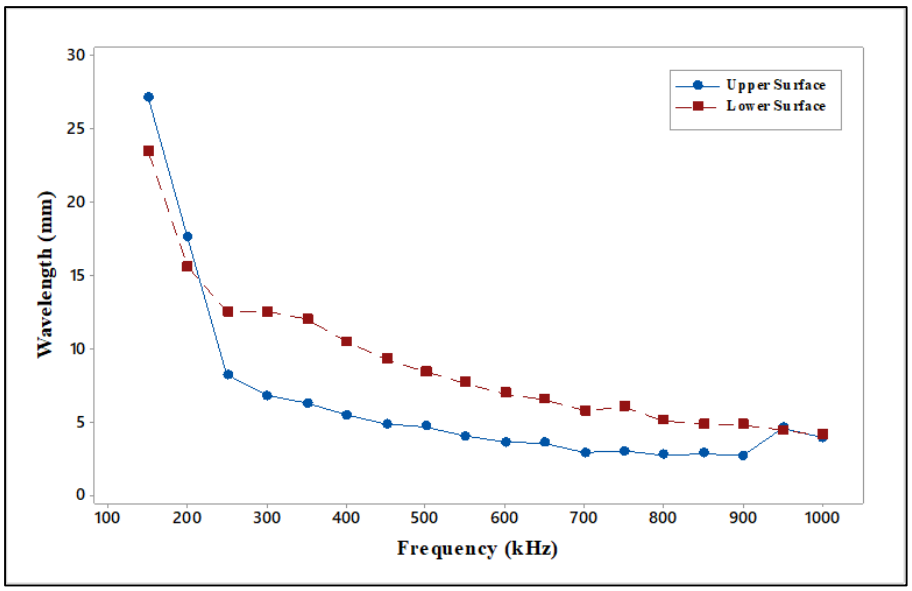


**Figure 8** Wavelength as a function of frequency

### 3.2. Attenuation in AU technique testing

In any materials, attenuation occurs as a result of the absorption and scattering of energy when the wave propagates through the medium. The peak amplitudes of the received signal at 60 mm and 120 mm sensor spacing were used to calculate the attenuation in the isotropic material, as a function of frequency in the isotropic material. A total of 18 measurements were obtained at each position for both upper and lower surfaces at each frequency to increase accuracy. Then Eq. (1) was incorporated to get the attenuation coefficient.

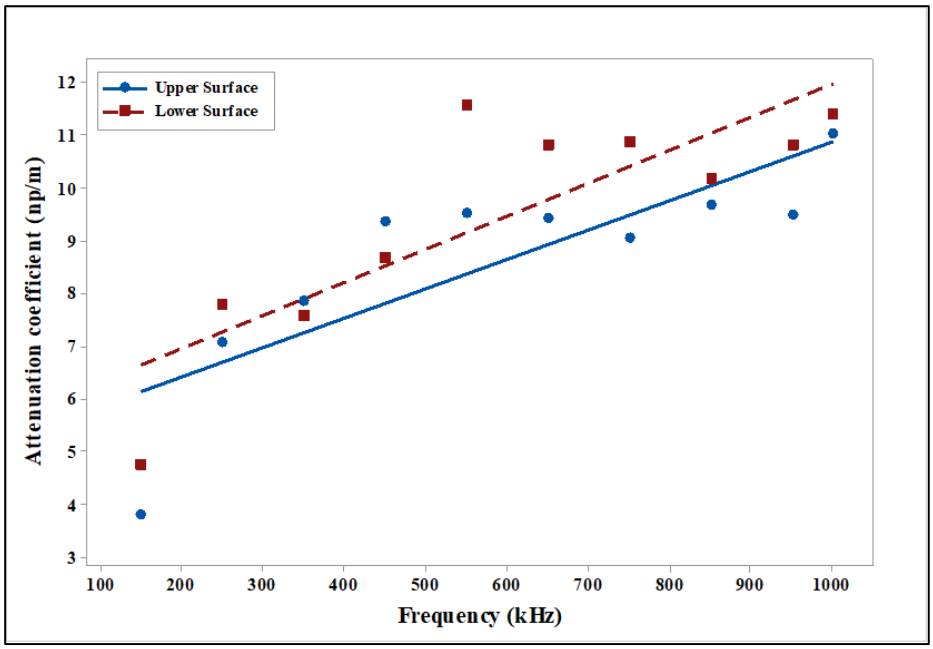


**Figure 9** Attenuation coefficient as a function of frequency for implementing AU technique for an isotropic Al6082-T6 material

Fig. 9 shows that the obtained attenuation coefficient was dependent on the frequency being monitored. An assessment of linear regression was carried out on the data for both surfaces as shown in Fig. 9. There was a linear relationship between the attenuation coefficient and the frequency, based on the information. The attenuation coefficient rises as the frequency of the signal increases.

## 4. Conclusions

AU wave propagation in an isotropic Al 6082-T6 plate has been experimentally and analytically investigated. With the implementation of the AU technique to the aluminium specimen, the primary wave generated was a symmetric Lamb wave. Attenuation played a significant role during the experimentation, because it was evident that peak amplitude decreased with an increase in the frequency. This established that plate waves could be generated with the application of AU technique. A plate wave with a wavelength as short as 3.92 mm for the specimen could be created without considerable dispersion, up to 1 MHz.

Finally, the experimental wave velocity curve followed the predicted trend by the analytical model, though there was a variation of 6.7% numerically. However, the symmetric plate waves were appreciably non-dispersive. Therefore, it can be concluded that AU technique generated a Lamb/plate waves without dispersion, which was desired. The attenuation increased with the frequency, showing the influence of reflection of waves from the plate's edges.

## Compliance with ethical standards

### *Acknowledgments*

This research was funded by DTA3/H2020 as a part of COFUND programme with University of Hertfordshire through University Alliance Scheme and as the host.

### *Disclosure of conflict of interest*

The authors declare that they have no known competing financial interests or personal relationships that could have appeared to influence the work reported in this paper.

### *Authors' statement*

All persons who meet authorship criteria are listed as authors, and all authors certify that they have participated sufficiently in the work to take public responsibility for the content, including participation in the concept, design, analysis, writing and/or revision of the manuscript. This statement is signed by all the authors.

## References

[1] Wang L, Yuan FG. Group velocity and characteristic wave curves of Lamb waves in composites: Modeling and experiments. Compos Sci Technol 2007;67:1370–84. https://doi.org/10.1016/J.COMPSCITECH.2006.09.023.

[2] Spyrou ED, Tsenis T, Kappatos V. Acousto-ultrasonic analysis of defects in composite specimens used in transportation domain. J Meas Eng 2021;9:117–27. https://doi.org/10.21595/JME.2021.21932.

[3] Vary A. The Acousto-Ultrasonic Approach. Acousto-Ultrasonics 1988:1–21. https://doi.org/10.1007/978-1-4757-1965-9_1.

[4] Sun CT, Achenbach JD, Herrmann G. Time-Harmonic Waves in a Stratified Medium Propagating in the Direction of the Layering. J Appl Mech 1968;35:408–11. https://doi.org/10.1115/1.3601212.

[5] Hemann JH, Baaklini GY, Baaklini GY. The effect of stress on ultrasonic pulses in fiber reinforced composites 1983.

[6] Viktorov IA (Igor' A. Rayleigh and Lamb waves: physical theory and applications. 1967:154.

[7] Lamb FRS. On waves in an elastic plate. Proc R Soc London Ser A, Contain Pap a Math Phys Character 1917;93:114–28. https://doi.org/10.1098/RSPA.1917.0008.

[8] Bond LJ, Saffari N. Crack Characterisation in Turbine Disks. Rev Prog Quant Nondestruct Eval 1984;3 A:251–62. https://doi.org/10.1007/978-1-4684-1194-2_23.

[9] Fahr A, Johar S, Murthy MK, Sturrock WR. Surface Acoustic Wave Studies of Surface Cracks in Ceramics. Rev Prog Quant Nondestruct Eval 1984;3 A:239–49. https://doi.org/10.1007/978-1-4684-1194-2_22.

[10] Lowe MJ. Matrix Techniques for Modeling Ultrasonic Waves in Multilayered Media. IEEE Trans Ultrason Ferroelectr Freq Control 1995;42:525–42. https://doi.org/10.1109/58.393096.

[11] Guo N, Cawley P. Lamb wave propagation in composite laminates and its relationship with acousto-ultrasonics. NDT E Int 1993;26:75–84. https://doi.org/10.1016/0963-8695(93)90257-U.

[12] Habeger CC, Mann RW, Baum GA. Ultrasonic plate waves in paper. Ultrasonics 1979;17:57–62. https://doi.org/10.1016/0041-624X(79)90096-9.

[13] Datta SK, Chimenti DE. Elastic Waves in Composite Media and Structures: With Applications to Ultrasonic Nondestructive Evaluation . J Acoust Soc Am 2009;126:1633–4. https://doi.org/10.1121/1.3180131.

[14] Spytek J, Ziaja-Sujdak A, Dziedziech K, Pieczonka L, Pelivanov I, Ambrozinski L. Evaluation of disbonds at various interfaces of adhesively bonded aluminum plates using all-optical excitation and detection of zero-group velocity Lamb waves. NDT E Int 2020;112:102249. https://doi.org/10.1016/J.NDTEINT.2020.102249.

[15] Worlton DC, Frederick CL. ULTRASONIC METHOD OF MEASURING THICKNESS USING LAMB WAVES 1964.

[16] Worlton DC. Experimental Confirmation of Lamb Waves at Megacycle Frequencies. J Appl Phys 2004;32:967. https://doi.org/10.1063/1.1736196.

[17] Rose JL. Ultrasonic Guided Waves in Solid Media. Ultrason Guid Waves Solid Media 2014;9781107048:1–512. https://doi.org/10.1017/CBO9781107273610.

[18] Nair A, Cai CS. Acoustic emission monitoring of bridges: Review and case studies. Eng Struct 2010;32:1704–14. https://doi.org/10.1016/j.engstruct.2010.02.020.

[19] Sve C. Time-Harmonic Waves Traveling Obliquely in a Periodically Laminated Medium. J Appl Mech 1971;38:477–82. https://doi.org/10.1115/1.3408800.

[20] Whittier JS, Peck JC. Experiments on Dispersive Pulse Propagation in Laminated Composites and Comparison With Theory. J Appl Mech 1969;36:485–90. https://doi.org/10.1115/1.3564705.

[21] Peck JC, Gurtman GA. Dispersive Pulse Propagation Parallel to the Interfaces of a Laminated Composite. J Appl Mech 1969;36:479–84. https://doi.org/10.1115/1.3564704.

[22] Scheuer C, Boot E, Carse N, Clardy A, Gallagher J, Heck S, et al. WAVES AND VIBRATIONS IN DIRECTIONALLY REINFORCED COMPOSITES. Compos Mater 1974;v:309–51. https://doi.org/10.2/JQUERY.MIN.JS.

[23] Kohn W. Propagation of Low Frequency Elastic Disturbances in a Three-Dimensional Composite Material. J Appl Mech 1975;42:159–64. https://doi.org/10.1115/1.3423508.

[24] Tsirogiannis EC, Stavroulakis GE, Makridis SS. Electric car chassis for Shell Eco Marathon competition: Design, modelling and finite element analysis. World Electr Veh J 2019;10. https://doi.org/10.3390/WEVJ10010008.

[25] Payan C, Ulrich TJ, Le Bas PY, Saleh T, Guimaraes M. Quantitative linear and nonlinear resonance inspection techniques and analysis for material characterization: Application to concrete thermal damage. J Acoust Soc Am 2014;136:537–46. https://doi.org/10.1121/1.4887451.

[26] Sarr CAT, Chataigner S, Gaillet L, Godin N. Nondestructive evaluation of FRP-reinforced structures bonded joints using acousto-ultrasonic: Towards diagnostic of damage state. Constr Build Mater 2021;313:125499. https://doi.org/10.1016/J.CONBUILDMAT.2021.125499.

[27] Kiernan MT. A physical model for the acousto-ultrasonic method 1989.

[28] Moon SM, Jerina KL, Hahn HT. Acousto-Ultrasonic Wave Propagation in Composite Laminates. Acousto-Ultrasonics, Springer US; 1988, p. 111–25. https://doi.org/10.1007/978-1-4757-1965-9_8.

[29] Masserey B, Fromme P. In-situ monitoring of fatigue crack growth using high frequency guided waves. NDT E Int 2015;71:1–7. https://doi.org/10.1016/J.NDTEINT.2014.12.007.

[30] Masserey B, Fromme P. Surface defect detection in stiffened plate structures using Rayleigh-like waves. NDT E Int 2009;42:564–72. https://doi.org/10.1016/J.NDTEINT.2009.04.006.